Secondary structure of silaffin at interfaces and titania formation

Eugenia Kharlampieva, Chang Min Jung, Veronika Kozlovskaya and Vladimir V. Tsukruk*

We report on the secondary structure of the recombinant silaffin protein, rSilC, at liquid–solid and air–solid interfaces with polyelectrolyte layer-by-layer (LbL) films serving as templates to mediate protein adsorption. By exploiting *in situ* ATR-FTIR spectroscopy directly we revealed that the molecular layer of rSilC adsorbed on the LbL surface exhibits a random coil conformation in a hydrated state. In contrast, the partial transition into β-sheet state is observed when the protein is deposited by spin casting with fast water removal. Both forms of rSilC surface layers are capable of mineralization of titania nanostructures at ambient conditions. We suggest that the careful tailoring of the silaffin secondary structure both at interfaces and in solution with particular amino acid sequences capable of intra- and inter-molecular transformations is essential for directing the "bio-titania" mineralization resulting in nanoparticles to large microstructures.

Introduction

Adaptive and responsive hybrid nanomaterials made of organic (synthetic or biological) matrices and inorganic nanostructures with unique physical properties (optical, conductive, magnetic) are of interest for various advanced applications in bio- and nanotechnology.[1,2] Such organic–inorganic nanomaterials can be designed either by adding inorganic nanofillers into soft matrices or by the direct synthesis of inorganic nanostructures inside these soft matrices with proper functionalities (*e.g. via* reduction of metal ions).[3,4] In contrast to the traditional synthesis methods, nanostructure synthesis with assistance of biological materials offers ambient conditions and therefore, presents a simple, environmentally friendly, but powerful tool in creating hybrid materials with novel properties and functions.[5–7] The enormous interest in developing protein-based materials is due to the unique "polymer" chemistry of biomolecules, such as mono-dispersity and the ability to predetermine a polymer-chain length and the exact sequence of "monomers".[8] In addition, the protein ability to form complex secondary structures and undergo conformational changes allows for a broad variation of bio-enabled conditions for obtaining different types of nano-structures at ambient environment.

One of the recent examples of proteins, which are involved in bio-enabled synthesis of nanomaterials, is silaffin. First identified in diatoms, silaffins, represent a class of peptides and proteins directing precipitation of silica at neutral pH and ambient temperatures *in vitro*.[9] In addition to silica formation, silaffin has been recently recognized as an attractive template for titania mineralization under mild aqueous conditions.[10,11] These titania nanostructures are of special importance due to their current and prospective applications as photocatalysts, UV blockers, photochromic pigments, oxygen sensors and components in lithium batteries and solar cells.[12] Titania nanostructures are mostly synthesized in solutions in the presence of biomolecules,

involving silicateins, silaffin proteins and peptides, lysozyme, and individual amino acids.[13–20] Much less is known about a bio-enabled titania formation on solid templates with different functionalities.[21,22] For instance, titania was generated on bio-engineered flagella of mesophilic bacteria or living diatoms.[21,23] Silk–titania films with uniformly dispersed titania nanoparticles have been generated using a sol–gel method, while 3D titania–ferritin microstructures have been obtained by mineralization of titania-binding peptides.[22,24]

The major challenge in surface-mediated bio-enabled synthesis of inorganic nanostructures is fine control of protein adsorption, stability, and resulting conformation at interfaces. The protein hydrophobicity and charges, surface chemistry and the presence of contacting proteins, non-covalent interactions, initial protein conformations, hydrated state and dehydration have all been shown to contribute to the adsorption process.[25,26] In the case of surface-mediated protein-induced mineralization, the way to bring proteins to surfaces should be versatile, simple, robust, and should not result in loss of protein activity towards synthesis of inorganic nanostructures.

One promising technique that has widely been used to create protein–polymer surface layers with controlled morphology is based on LbL assembly.[27–32] The technique, first developed as sequential assembly of linear synthetic polyelectrolytes of opposite charge, was then transferred to other molecules including biomolecules and nanoparticles.[33–35] Surface engineering with LbL assembly allows for an effective control over proteins adsorption by varying the pH in a region close to the isoelectric point of the protein. This way, proteins are adsorbed on or encapsulated into polycation/polyanion LbL films.[36–41] In this case, the presence of polyelectrolytes was found to significantly impact conformational changes in proteins.[42–45] In this aspect, Attenuated Total Reflection Fourier transform infrared spectroscopy (ATR-FTIR) was used as a powerful technique, which allowed resolution of protein secondary structures even within a single molecular layer at solid–liquid or solid–air interfaces.[46,47] It has been shown that LbL-modified substrates can create a favorable environment for incorporated

School of Materials Science and Engineering, Georgia Institute of Technology, Atlanta, GA, 30332, USA. E-mail: Vladimir@mse.gatech.edu

biomolecules resulting in a preservation of their secondary structures and functions.[33,43,45,48,49] For example, preserving bovine serum albumin (BSA) and hen egg white lysozyme (HEL) secondary structures was observed when the proteins were deposited on a negatively charged poly(sodium 4-styrenesulfonate) (PSS).[43] On the other hand, the secondary structure can be altered upon deposition on an oppositely charged poly(allylamine hydrochloride) (PAH) surface, resulting in a decrease in the α-helix content and an increase in intramolecular β-structures. However, despite recent progress made in investigating protein conformations at interfaces, the current studies are mostly focused on globular proteins or polypeptides but the surface behavior of silaffins has remained uncharted to date.

In this study, we discuss the mechanism of surface-mediated silaffin-enabled formation of titania nanostructures by focusing on rSilC conformational state at liquid–solid and air–solid interfaces. We study secondary structure of adsorbed silaffin and its variation in the course of titania formation at a solid–liquid interface, a rarely addressed but practically important case. This work is triggered by our recent results which have demonstrated that rSilC adopted a mixture of β-sheets and random coils after being spin-cast on polyelectrolyte surfaces leading to the formation of uniform 6 nm titania nanoparticles.[50,51] It has been suggested that the conformational transition is crucial for the formation of individual nanopartciles on surfaces in contrast to the microscopic aggregates reported in solutions.[10,20,50] However, understanding the mechanism of titania biomineralization requires investigation of how the silaffin conformation at a liquid–solid interface is affected by a polyelectrolyte template. In this respect, there are some important questions which will be addressed in this study. How does the interface control protein structure? What is the role of assembly conditions in silaffin conformational transition? What are the main silaffin groups responsible for the random-coil to β-sheet transitions? How do the silaffin deposition conditions effect its mineralization activity on surfaces?

Experimental

Materials

Poly(allylamine hydrochloride) (PAH, M_w = 65 000), and poly(sodium 4-styrenesulfonate) (PSS, M_w = 70 000), Titanium(v) bis(ammonium lactato) dihydroxide (TIBALDH) were purchased from Aldrich. The recombinant silaffin rSilC (17 625 Da) was prepared as described previously.[10] Nanopure water with a resistivity 18.2 MΩ cm was used in all experiments. D_2O with 99.9% isotope content was purchased from Cambridge Isotope Laboratories and was used as received. To control pH and ionic strength, concentrated HCl and inorganic salts NaCl, Na_2HPO_4 and NaH_2PO_4 (General Storage, pure grade) were used as received.

ATR-FTIR measurements

LbL assembly, rSilC deposition and mineralization were monitored by infrared spectroscopy using ATR-FTIR. The ATR-FTIR spectra were collected using a Bruker Fourier transform infrared (FTIR) spectrometer (Vertex 70) equipped with a narrow-band mercury cadmium telluride detector. The internal compartment of the FTIR spectrometer containing the liquid cell was purged with dry nitrogen. The ATR surface was a rectangular (50 mm × 10 mm × 2 mm) trapezoidal Ge or Si crystal (Harrick Scientific). Spectra were collected at 4 cm⁻¹ resolution, and the number of averaged scans was 120. To obtain the absorbance spectra analyzed below, each spectrum was corrected to the corresponding background, measured for the same ATR cell with the same D_2O buffer solution. The bare ATR crystal was used as a background. To eliminate an overlap of the IR spectra of polyacids and proteins in the 1700–1500 cm⁻¹ region with the strong water band, D_2O was used as a solvent. D_2O with 99.9% isotope content was purchased from Cambridge Isotope Laboratories.

Multilayer films of (PSS–PAH)$_n$ were deposited on a hydrophilic Ge or Si crystal *in situ* within the flow-through ATR-FTIR liquid cell obtained from Harrick Scientific. Multilayer deposition was performed as described elsewhere.[47] Briefly, 0.1 mg mL⁻¹ solutions of PAH in 0.01 M buffer solution was allowed to adsorb onto the surface of an oxidized Ge crystal at pH 7 for 10 min, and after that the polymer solution was replaced by the buffer solution without polymer. PSS was then deposited from 0.1 mg mL⁻¹ solution in the same buffer and the deposition cycle was repeated. To prepare a wet rSilC film *in situ*, the silaffin was adsorbed onto the PSS-coated surface from 0.5 mg mL⁻¹ solution at pH 7 in the liquid cell and remained at the solid–water interface for the conformational and mineralization study. To encapsulate rSilC within the LbL matrix, PSS was deposited on top of the rSilC film followed by sequential deposition of additional LbL layers.

To fabricate spin-cast surface layers, the silaffin was adsorbed on top of the ATR Ge crystal pre-coated with a 2-bilayer PAH–PSS film. The D_2O solution of rSilC (1.5 mg mL⁻¹) was dropped on one side of the crystal and rotated until dried, followed by rinsing with water. The spectrum of the film was then taken in a dry flow-trough cell with a spectrum of the dry clean Ge crystal taken as a background.

Titania nanostructures formation on the rSilC surfaces were performed *in situ* by filling the cell with 0.2 M TIBALDH solution in 0.05 M phosphate at pH 7 in a D_2O solution, keeping the crystal exposed to the solution for 7 days followed by extensive rinsing with the buffered D_2O solution. The solution spectrum of rSilC was obtained in the liquid cell by bringing a 10 mg mL⁻¹ silaffin solution in a contact with a non-adsorbing surface. For that purpose, Ge crystal was pre-coated with a PAH layer to prevent silaffin deposition. The absorption peaks were baseline-corrected and analyzed with Galactic Grams/32 software using curve-fitting.[47] The relative contribution of the spectra components was obtained by integration of the band areas. In the fitting procedure the wavenumbers, widths and Gaussian band profiles were fixed, but peak intensities were varied for different spectra.

Multilayer deposition and titania synthesis on silicon wafers

Multilayer films and protein deposition on silicon wafers were fabricated by spin-assisted LbL (SA-LbL) method, which is a combination of spin-assisted and conventional LbL techniques.[52] Specifically, 30 μL of 1 mg mL⁻¹ polyelectrolyte solutions were sequentially dropped on the silicon substrate, rotated

for 20 s with a 5000 rpm rotation speed (Laurell), and rinsed twice with H_2O between the deposition cycles. rSilC was then deposited from 1.5 mg mL^{-1} solution on the polyelectrolyte film. Unbound protein was removed by extensive rinsing with H_2O. Formation of titania nanoparticles was achieved by exposure of the rSilC film to 0.2 M TIBALDH solution in 0.05 M phosphate for 7 days at 24 °C in the dark, followed by extensive rinsing with H_2O.

Instrumentation

Protein deposition and titania formation on silicon wafers were monitored by AFM (Dimension 3000 microscope, Digital Instruments). AFM images were collected in the tapping mode with silicon tips with a spring constant of 50 N m^{-1} in according to usual procedures adapted in our laboratory.[53] AFM imaging in tapping mode under fluid was performed on a MultiMode (NanoScope IIIa) microscope (Veeco Metrology) equipped with a fluid cell.[54] Ellipsometry measurements of layer thicknesses were performed by using a M2000U (Woolam) spectroscopic ellipsometer. Energy dispersive X-ray spectroscopy (EDX) (INCA energy dispersive X-ray spectrometer) measurements were conducted with a scanning electron microscope (SEM) S-3400M (Hitachi). Surface Enhanced Raman Spectroscopy (SERS) was performed with a CRM-200 confocal Raman microscope (Witec) in a back-scattered geometry with 100× objective lens.[55] The excitation laser is argon-ion laser with wavelength of 514.5 nm and the incident power is below 1 mW. Surface enhancement was provided by 12 nm silver nanoparticles drop-cast on glass slides prior rSilC deposition and titania growth.

Molecular modeling

For the analysis of rSilC 3D structure, Materials Studio was exploited.[56] As the first step, amino acid sequences were built using the Visualizer module and its geometry optimized through the energy minimization tool in the Discover module using the PCFF force field and the Smart Minimizer tool.[56] Second, the amino sequence information which can be changed to the β-sheet structure was analyzed by Jpred program with its secondary prediction accuracy over 81%.[57,58] The program incorporates the Jnet algorithm which makes the prediction accuracy more precise. FASTA files which included the sequences of single or multiple sequences (single, two and fifteen) rSilC proteins were made and analyzed.[59]

Results

Conformational transitions of rSilC as followed by *in situ* ATR-FTIR

The molecular structure of the silaffin is shown in Fig. 1. The main hydrophilic functional groups of rSilC are presented by lysine and arginine amino acids, which make the protein highly cationic with isoelectric point, pI, of 11.8.[10] To assure robust surface tethering of the positively charged rSilC, the silicon wafer was pre-coated with a (PAH–PSS)$_2$ LbL film with a negatively charged PSS as a top layer. PSS is a strong polyelectrolyte whose charge does not depend on pH, and PAH is a polybase that behaves as a strong permanently charged polyelectrolyte in acidic and neutral media.[47] Our previous findings showed that rSilC undergoes a transformation from a random-coil conformation in solutions into a mixed secondary structure with both random coil
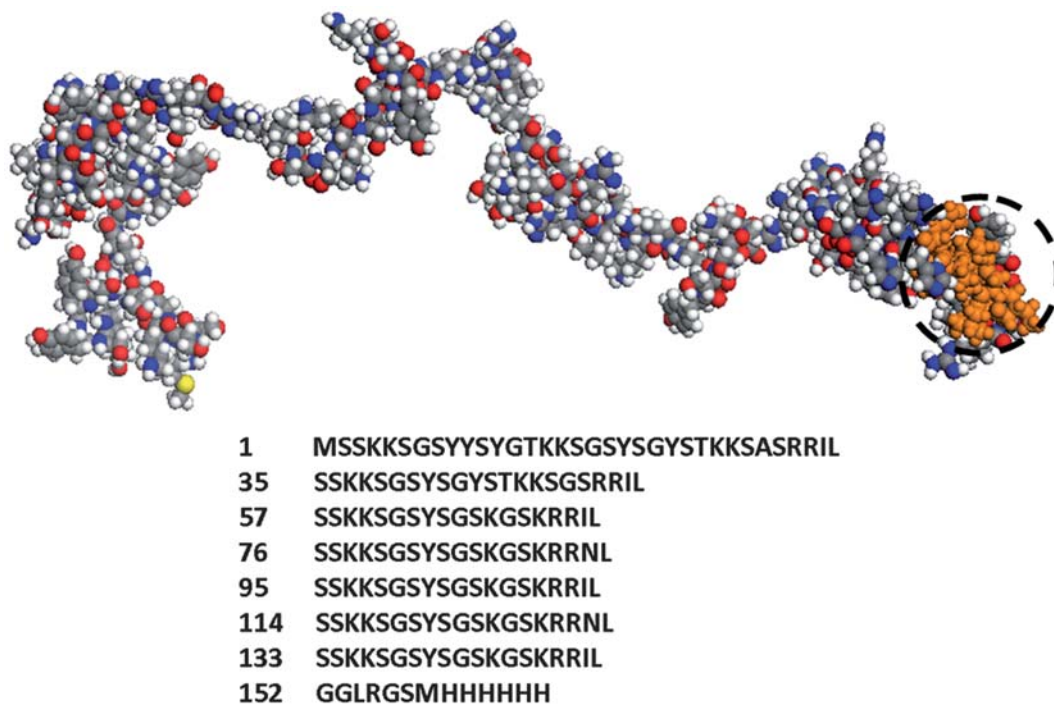

1	MSSKKSGSYYSYGTKKSGSYSGYSTKKSASRRIL
35	SSKKSGSYSGYSTKKSGSRRIL
57	SSKKSGSYSGSKGSKRRIL
76	SSKKSGSYSGSKGSKRRNL
95	SSKKSGSYSGSKGSKRRIL
114	SSKKSGSYSGSKGSKRRNL
133	SSKKSGSYSGSKGSKRRIL
152	GGLRGSMHHHHHH

Fig. 1 A computer simulated 3D molecular model structure of a recombinant silaffin with β-sheet-forming segment shown by a circle. The protein sequence is presented by the one letter amino acid code.[10] The circle highlights the amino acid motif ILGGLRGSMH capable of forming intra-molecular β-sheets.

and β-sheets present when spin-cast on solid–air interfaces.[50] To get insight into the rSilC structural transformations at solid–liquid interfaces we deposit silaffin *in situ* in a flow-trough liquid cell which prevents the film from being exposed to air during adsorption.

Fig. 2A demonstrates the ATR-FTIR spectra of rSilC in a D_2O solution and after deposition as a single layer onto a modified surface in a liquid cell at pH 7. One sees that the robust rSilC surface layer is formed at the solid–water interface as a result of electrostatic interactions between the protein amino-groups and oppositely charged sulfonate-groups of PSS. Our results on the rSilC adsorption correlate well with the earlier works on interactions of biomolecules with polymeric surfaces, which showed that protein–polyelectrolyte interactions are mainly of electrostatic origin and protein binding strongly depends on the charge of the underlying layer.[42,47,60] The FTIR spectrum also shows that the hydrated protein layer contains only random coil conformations (Fig. 2A). Indeed, the FTIR spectra of the hydrated rSilC layer is identical to that in solution as they both indicate the amide I bands centered at 1644 cm^{-1}, which is consistent with a random coil conformations for proteins (Fig. 2A).[61,62] The amide I band in proteins (1600–1700 cm^{-1}) is usually associated with C=O stretching vibrations in the protein backbone coupled to the N–H bending and C=N stretching modes.[47] The results for the hydrated films are in
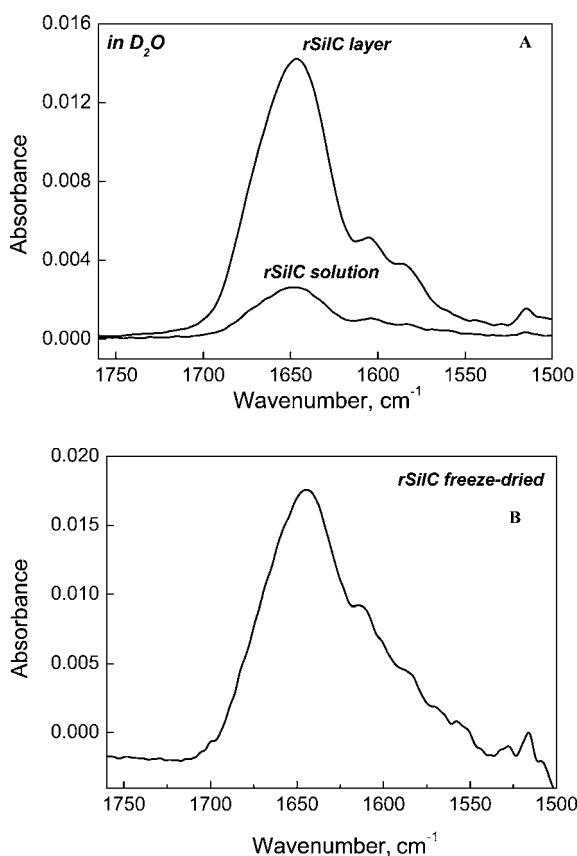
striking difference to those previously observed for dehydrated protein layers which showed high content of β-sheets with a strong peak at 1618 cm^{-1}.[43,50,61–63]

Surprisingly, the random-coil conformation for the hydrated rSilC films is preserved upon further slow removal of water and further dehydration of the protein surface layer. No changes in the spectrum of the random-coiled rSilC were observed after a treatment of the surface layer with dry nitrogen (not shown). Moreover, the freeze-dried rSilC obtained in powder by lyophilization of protein solution also indicates only random coil conformation (Fig. 2B).

Imbedding rSilC in a multilayer matrix

To further study the effect of polyelectrolyte films on silaffin secondary structure, rSilC was imbedded within LbL films by sequential assembly of rSilC with the oppositely charged PSS or with (PSS–PAH)$_n$ layers. Fig. 3 illustrates evolution of *in situ* ATR-FTIR spectra in rSilC–PAH–PSS system during deposition of the film in D_2O solutions at pH 7. We followed the polyelectrolyte deposition by observing PSS vibrational bands centered at 1600, 1036 and 1009 cm^{-1}.[64] As seen from Fig. 3, rSilC deposited on 3-bilayer PSS–PAH film was successfully coated with the PSS layer with no mass loss for the protein layer. Protein retains within the film after adding a topmost 3-bilayer PSS–PAH film (Fig. 3).

Fig. 4 demonstrates *in situ* monitoring of a sequential deposition of a two-component (rSilC–PSS)$_5$ multilayers directly on the surface of an ATR crystal. The intensity of amide I and II bands consistently increases with the deposition number, indicating a successful rSilC–PSS film growth, which is caused by charge-to-charge compensation between positive rSilC and negative PSS component. Inset in Fig. 4 shows that the thickness of the dry (rSilC–PSS)$_5$ film also linearly increases with the layer number which indicates the consistent film growth with no excessive protein diffusion inside the polymeric matrix.

The spectra of the imbedded proteins do not show any changes in amide I and amide II regions thus indicating that interactions
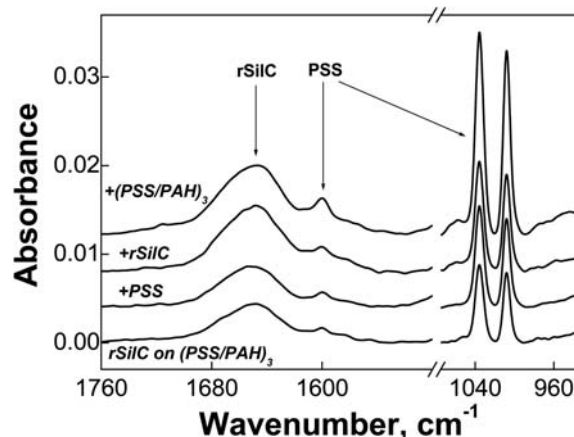

Fig. 2 (A) ATR-FTIR spectra of rSilC in the hydrated state in a D_2O solution and deposited from the solution on a PSS-terminated surface of a Si ATR crystal at pH 7. (B) The spectrum of an rSilC powder obtained after lyophilization of the silaffin solution.

Fig. 3 Embedding rSilC within PAH–PSS multilayers as monitored by *in situ* ATR-FTIR. The film was deposited on a Ge ATR crystal from a D_2O solution at pH 7. Arrows point to vibrational peaks associated with rSilC amide I band centered at 1645 cm^{-1} and to PSS absorption bands at 1602, 1035, and 1008 cm^{-1}.
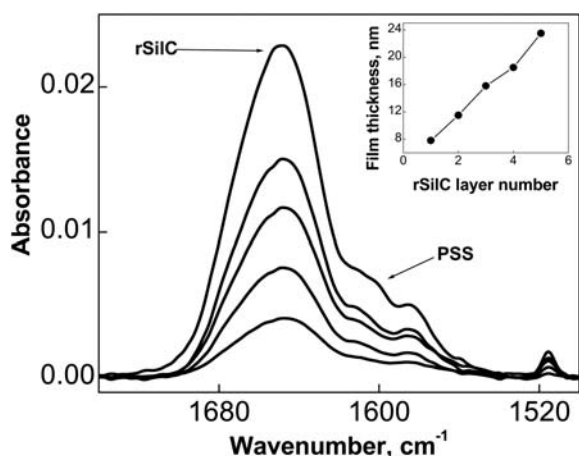
Fig. 4 Sequential deposition of a multilayer rSilC–PSS film at pH 7 from D$_2$O buffer solution as monitored by *in situ* ATR-FTIR. An ATR Si crystal was pre-coated with a 2-bilayer (PAH–PSS) film and this prime film was taken as a background. Inset shows the evolution of film thickness as a function of a layer number.

with both underlying and capping polyelectrolyte layers do not affect the protein secondary structure after deposition. Therefore, the LbL multilayers can "freeze" the random coil structure of silaffin from any structural changes after deposition/imbedding regardless strong electrostatic interactions between the silaffin and the adjacent PSS, a situation observed for protein–polymer surface complexes.[45,65]

Titania mineralization

As was found earlier, the interaction of the negatively charged TIBALDH molecules with the positively charged rSilC resulted in amino-group catalyzes hydrolysis of the TIBALDH-precursor followed by precipitation of microscopic titania structures from solutions.[9,10,19] The similar mechanism was also proposed for rSilC-induced growth of titania nanoparticles inside the protein domains when silaffin was spin-cast on the solid–air interface.[50,51]
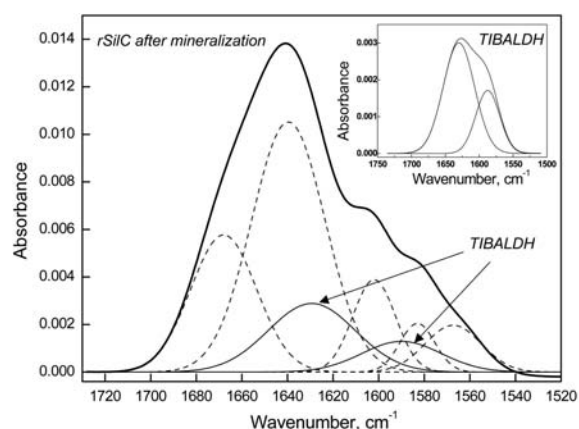

Fig. 5 Deconvolution of a ATR-FTIR spectrum of rSilC surface layer after exposure to a TIBALDH solution for 7 days. Arrows point to the vibrational peaks associated with TIBALDH. Inset shows a spectrum of TIBALDH adsorbed on a PAH-terminated surface. The films were deposited on a Si ATR crystal from D$_2$O solution at pH 7.

Fig. 5 shows an ATR-FTIR spectrum of rSilC surface layer after incubation with TIBALDH precursor in phosphate buffer for a week. The spectrum deconvolution reveals the presence of two major peaks in amide I region centered at 1664 cm^{-1} and 1642 cm^{-1} and associated with unordered turns and random coils, respectively.[50] The vibrational peaks in amide II region (1500–1600 cm^{-1}) are usually associated with N–H bending[47] and assigned to arginine side groups and tyrosine aromatic amino acids groups. In addition, two bands centered at 1630 and 1588 cm^{-1} are found in the spectrum and assigned to TIBALDH. The bands were introduced in the spectra of rSilC by keeping the TIBALDH band ratio and peak positions constant (see inset in Fig. 5). Thus, the result indicates no change in random coil conformation of silaffin surface layers after association with TIBALDH and titania mineralization. This is in contrast to dramatic changes in protein conformation usually observed for proteins in the course of biomineralization.[66] For instance, the interaction of poly-L-lysine (PLL) with silica precursors in solutions results in a conversion of the random coil conformation into helical one, which gives rise to hexagonal silica in contrast to the silica spheres induced by β-sheet structured PLL.[66]

One can expect that the incubation or rSilC with TIBALDH at room temperature can induce protein denaturation.[67] However, in a control experiment with rSilC monolayer exposed to phosphate buffer for a week at pH 7, the spectrum of rSilC did not reveal any changes with time, which indicates stability of the adsorbed protein layer at the mineralization conditions (data not presented).

To further investigate the effect of silaffin conformation on its mineralization activity we perform AFM study of the rSilC layer in the hydrated and dry states. Fig. 6 shows the topographical image of a hydrated silaffin layer performed directly in a buffered solution. One can see that the random-coil protein forms the distinct surface domains which are stable in highly hydrated state (Fig. 6A). Moreover, the domains are well-separated and, thus should facilitate an easy TIBALDH binding followed by titania formation as will be discussed later in the paper (Fig. 6B).

The surface morphology of the hydrated 5 nm silaffin layer after drying is shown in Fig. 7A. The images demonstrate the well-developed grainy morphology with the surface microroughness (RMS) of 2.6 nm within 1×1 μm^2. The results are in contrast to our earlier findings on the spin-cast films, which represented a mixture of random-coil and β-sheet secondary structures, and demonstrated much lower microroughness of 0.5 nm.[50] Moreover, when the silaffin is in predominant random-coil state the rSilC domains are polydisperse and of 10 ± 6 nm in height, unlike the much smaller surface features of 1.6 ± 0.7 nm in height for the mixed silaffin state (Fig. 7A and B).

The difference in initial secondary structures of the two types of rSilC (random coil and random coil + β-sheet) initiated drastically different titania morphologies. Indeed, the microroughness for the titania-containing protein layer in random-coil state is found to be 6.2 nm, which much higher than that for the films with the mixed secondary structure (2.5 nm) (Fig. 7C and D). Correspondingly, the average dimension of titania nanoparticles grown on the random-coil rSilC is 25 ± 13 nm in contrast to the 6.0 ± 1.5 nm diameter observed for the titania nanoparticles grown on mixed (random coils + β-sheets) protein layer (Fig. 7C and D). The AFM image of the titania grown on
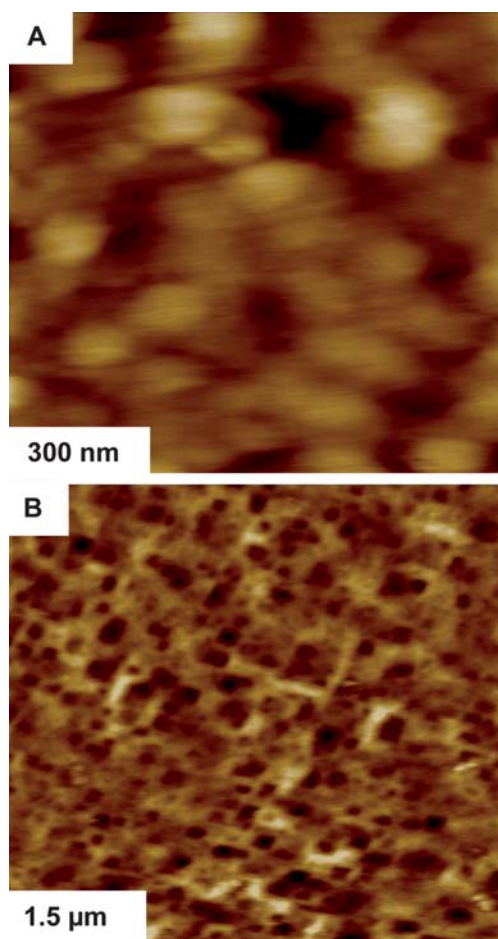
Fig. 6 AFM topographical images of rSilC layer under fluid. Height is 15 nm (A), 50 nm (B).
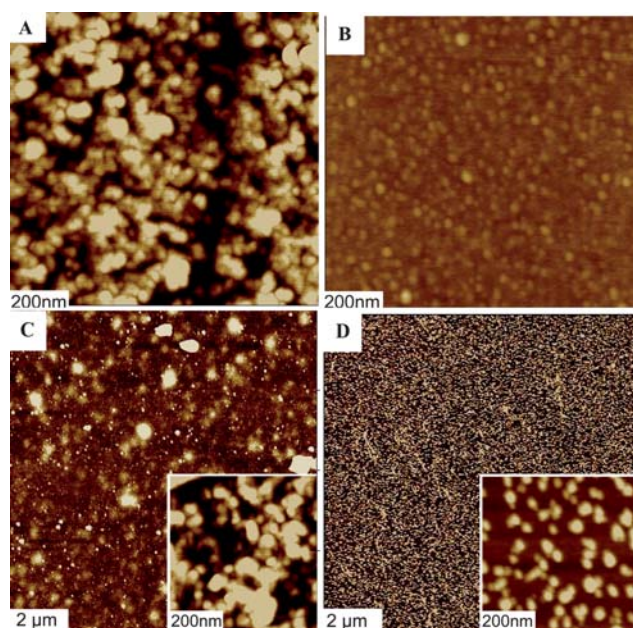

Fig. 7 AFM topographical images of the dry films of rSilC in a random-coil conformation (A) and in the mixed (random coils + β sheets) state (B). TiO$_2$ nanostructures grown on the random-coil rSilC (C) and on the mixed (random coils + β sheets) rSilC (D). Height is 10 nm for all images.

the mixed-conformation rSilC also confirms their exceptional uniformity (Fig. 7D). This is in contrast with microscopic aggregations of the titania structures grown on protein layers with the random-coil state (Fig. 7C). The dramatic difference in the titania structures obtained in these two cases indicate that titania mineralization is significantly affected by the secondary structure of the initial silaffin surface layer.

The presence of mineralized titania induced by random-coiled rSilC was confirmed with EDX spectroscopy. The EDX spectrum reveals presence of Ti and O elements in the titania nanostructures (Fig. 8A). However, EDX does not provide input into phase state of titania phase. Thus, the titania phase was additionally examined with surface-enhanced Raman scattering (SERS), which has been shown to identify trace amount of materials and is sensitive to the local ordering.[68,69] The spectrum reveals three characteristic peaks centered at 410, 520, and 630 cm^{-1} associated with the titania (Fig. 8B). The positions of the peaks as well as their ratio of intensities are in good agreement with the earlier observed Raman scattering for ordered tinania nanostructures.[70,71] The spectrum also shows that titania nanoparticles are composed of the mixed amorphous–anatase phases. Indeed, the peaks are well-defined and clearly differ from a broad background, a characteristic for amorphous titania.[71] Thus, random-coil rSilC affords formation of the mixed (amorphous–anatase) titania similar to that found for the mixed (random coil + β sheet rSilC).[50] The latter indicates a capability of the surface-tethered protein of providing a certain level of
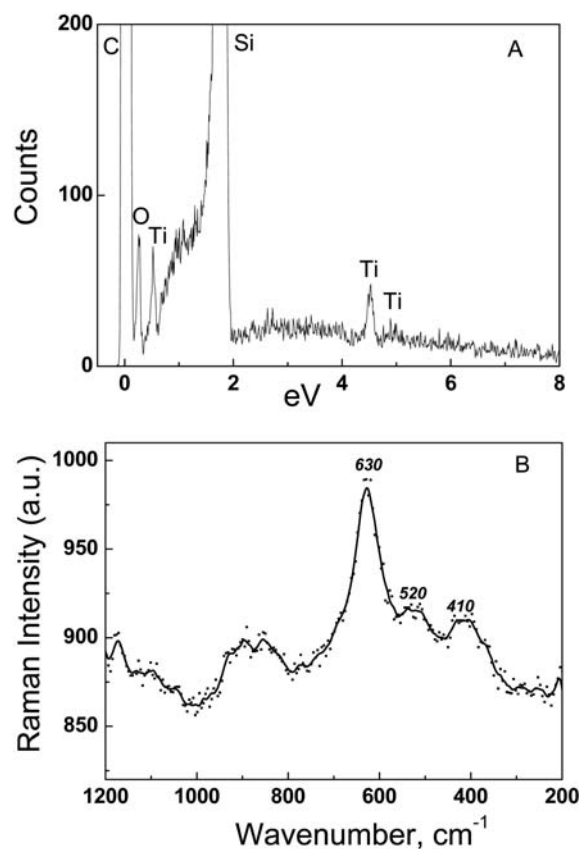

Fig. 8 EDX (A) and SERS (B) spectra of titania grown on a random-coil rSilC.

This journal is © The Royal Society of Chemistry 2010

J. Mater. Chem., 2010, **20**, 5242–5250 | 5247

ordering to the mineralized titania, which is partially crystalline, in contrast to the surface-attached synthetic polycations providing formation of amorphous titania at ambient conditions.[72]

Discussion

The ability of initially random-coil biomolecules to undergo structural transitions upon adsorption has been revealed earlier. For example, both poly-L-lysine (PLL) and silk fibroin possess random coil conformations in good solvents but show β-sheets in cast films upon heating, interaction with polyelectrolytes, or upon treatment with organic solvents.[61,73–78] Moreover, a molecular layer of silk fibroin preserves its native random-coil structure in the hydrated film at solid–water interface, but adopts a partial transition into β-sheets upon drying.[79]

Similar to silk materials, silaffin studied in this work preserves its native random coil conformation in the hydrated surface film (Fig. 2A). However, in contrast to silk, the random secondary structure remains stable even upon dehydration while dried. On the other hand, the random-coil transformation into the mixed state of random coil and β-sheet secondary structures occurs when rSilC is directly spin-cast at air–solid interfaces as a nanoscale (3 nm thick) surface layer.[50] However, the control experiment with the freeze-dried rSilC demonstrates that the protein does not undergo the structural transition remaining in its random-coil conformation upon drying from bulk solutions (Fig. 2B). In contrast, the dehydration of nanoscale surface layer in the course of spin-casting resulted in the closely packed neighboring molecular fragments under constrained conditions which promotes a hydrogen-bonding and β-sheets formation of some "prone" sequences.[79–81]

Molecular modeling provided an insight into the mechanism of the silaffin ability to structural transformations.[82,83] Predicted amino acid sequences capable of transformation into intra- and inter-molecular β-sheets are presented in Fig. 1 and 9,

respectively. The segment which can afford intramolecular β-sheets transformations is ILGGLRGSMH, which presents the hydrophobic part of the protein because of the presence of nonpolar isoleucine (I), leucine (L), and glycine (G) groups (Fig. 1). We identified additional six sequences capable of forming β-sheets through inter-molecular interactions: 9–11(YYS), 32–35(RILS), 54–57(RILS), 72–76(RRILS), 110–133(RRILS) as have been revealed considering interactions between two neighboring silaffin molecules (Fig. 9). The same sequences were found when 15 silaffin molecules were analysed as well (not shown). Hydroxyl functionalities of the serine (S) and tyrosine (Y) motifs are also found to significantly contribute to the silaffin conformational transition. Our results are in good correlation with the simulation data obtained for the silaffin-type R5 peptides which were found to assemble in solution due to the close proximity of the charged hydrophilic arginine residues (R) to the nonpolar isoleucine (I) and leucine (L) motifs.[83] This RRIL sequence was found to be crucial for the R5-indiced mineralization of silica.[83] Therefore, rSilC sequence contains functionalities and segments which afford its transformation into β-sheets in the spin-cast film.

In contrast, a "pre-formed" random secondary structure, when the hydrated film is slowly adsorbed from solutions, cannot be transformed to more compact β-sheet structures upon post-dehydration and formation of drop-cast films. We suggest that this transformation is suppressed because the hydrophilic amino acids, such as Y, K, R, remain solvated, which prevents them from a close association appropriate for β-sheet formation. In addition, the chain-to-chain proximity is restricted by the repulsion between the charged groups (K, R) in the solvated states. The constrained chain mobility and the limited capability to the reorganization after initial anchoring of positively charged silaffin to the oppositely charged polyelectrolyte surfaces can be other important causes for the preservation of native random secondary structure. In contrast, the rSilC dehydration resulting in the transition from random coils into β-sheets in spin-cast films would be more favorable for the ultrathin films comparable to the protein chain dimensions.

The secondary structure of silaffin is a key factor affecting the formation of titania nanostructures. Random secondary structures in the hydrated solution-adsorbed films resulted in formation of polydisperse, heterogeneous clusters of larger nanostructures and their aggregates. In contrast, the mixed (random + β-sheets) secondary structure results in the formation of individual and uniform titania nanoparticles with suppressed nanoparticle aggregation.

Conclusion

We have investigated the silaffin conformational state at interfaces and demonstrated that the secondary structure of the silaffin layer is controlled by the deposition conditions. The adsorbed silaffin preserves its native random coil structure at solid–water interface in the hydrated films. The conformation is also unchanged when the hydrated rSilC layer is encapsulated inside polyelectrolyte matrix. However, at a solid–air interface dehydration of the spin-cast films induces inter- and intra-chain interactions leading to partial transformation from random coil rSilC into β-sheets. We suggest that the conformational
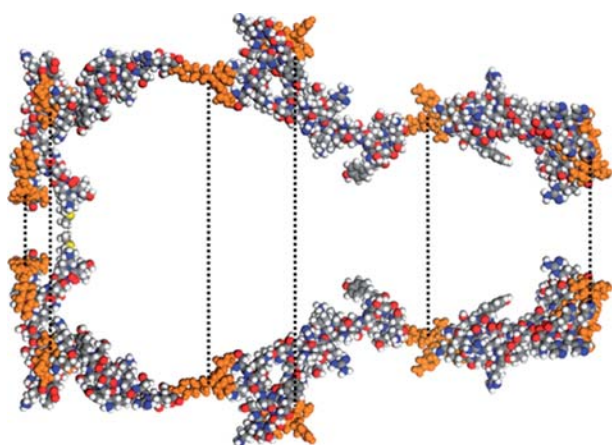

Fig. 9 Molecular model of transformation of random coil rSilC into a mixed secondary structure with intermolecular β-sheets. The amino acid motifs capable of forming parallel β-sheets are presented as 9–11(YYS), 32–35(RILS), 54–57(RILS), 72–76(RRILS), 110–113(RRILS), and 150–159(ILGGLRGSMH). Hydrogen-bonding interactions between the motifs are presented with dotted lines. Two neighboring molecules are separated for clarity.

transition is afforded by the close proximity of the polar arginine, serine, and tyrosine residues to the hydrophobic isoleucine and leucine motifs in course of fast and forced water removal from nanoscale protein film. In contrast, if slowly adsorbed as a random coil, rSilC preserves the random coil conformation upon further drying, indicating the surface capability to stabilize the initial random secondary structure. The rSilC secondary structure further controls morphology of the mineralized titania. The presence of β-sheets in the spin-cast silaffin layer promotes the formation of individual, uniformly dispersed titania nanoparticles, which is in striking contrast to the microscopic titania aggregates formed in the hydrated films with random coil structure. Both forms of rSilC (random or random + β-sheet) afford formation of mixed amorphous–anatase phases of titania nanoparticles. In addition to the fundamental interest in understanding of bio-titania synthesis *in vitro*, titania nanocomposites of a controlled morphology would be of importance for their potential applications in self-cleaning or photocatalytic structures.

Acknowledgements

References

1 (a) R. Sardar, A. M. Funston, P. Mulvaney and R. W. Murray, *Langmuir*, 2009, **25**, 13840; (b) K. Ariga, A. Vinu and M. Miyahara, *Curr. Nanosci.*, 2006, **2**, 197; (c) E. P. Giannelis, *Adv. Mater.*, 1996, **8**, 29; (d) E. L. Mayes, F. Vollrath and S. Mann, *Adv. Mater.*, 1998, **10**, 801.

2 (a) M. C. Stuart, W. Huck, J. Genzer, M. Müller, C. Ober, M. Stamm, G. Sukhorukov, I. Szleifer, V. V. Tsukruk, M. Urban, F. Winnik, S. Zauscher, I. Luzinov and S. Minko, *Nat. Mater.*, 2010, **9**, 101; (b) C. Jiang, S. Markutsya, Y. Pikus and V. V. Tsukruk, *Nat. Mater.*, 2004, **3**, 721; (c) I. Luzinov, S. Minko and V. V. Tsukruk, *Prog. Polym. Sci.*, 2004, **29**, 635; (d) I. Luzinov, S. Minko and V. V. Tsukruk, *Soft Matter*, 2008, **4**, 714; (e) M. E. McConney, K. D. Anderson, L. L. Brott, R. R. Naik and V. V. Tsukruk, *Adv. Funct. Mater.*, 2009, **19**, 2527.

3 (a) R. Naik, S. Stringer, G. Agarwal, S. Jones and M. Stone, *Nat. Mater.*, 2002, **1**, 169; (b) Y. Mang, H.-J. Kim, G. Vunjak-Novakovic and D. L. Kaplan, *Biomaterials*, 2006, **27**, 6064; (c) L. Qu, L. L. Brett, R. R. Naik, D. J. Pikas, S. M. Kirkpatrlck, D. W. Tomlin, P. W. Whitlock, S. J. Clarsen and M. O. Stone, *Nature*, 2001, **413**, 291; (d) Z. Tang, N. A. Kotov, S. Magonov and B. Ozturk, *Nat. Mater.*, 2003, **2**, 413; (e) S. Chang, S. Singamaneni, E. Kharlampieva, S. L. Young and V. V. Tsukruk, *Macromolecules*, 2009, **42**, 5781.

4 (a) C. Jiang, S. Markutsya, H. Shulha and V. V. Tsukruk, *Adv. Mater.*, 2005, **17**, 1669; (b) H. Ko, S. Chang and V. V. Tsukruk, *ACS Nano*, 2009, **3**, 181; (c) K. D. Anderson, J. M. Slocik, M. E. McConney, J. O. Enlow, R. Jakubiak, T. J. Bunning, R. R. Naik and V. V. Tsukruk, *Small*, 2009, **5**, 741; (d) V. Kozlovskaya, E. Kharlampieva, S. Chang, R. Muhlbauer and V. V. Tsukruk, *Chem. Mater.*, 2009, **21**, 2158; (e) R. Gunawidjaja, E. Kharlampieva, I. Choi and V. V. Tsukruk, *Small*, 2009, **5**, 2460; (f) S. Singamaneni, E. Kharlampieva, J.-H. Jang, M. E. McConney, H. Jiang, T. J. Bunning, E. L. Thomas and V. V. Tsukruk, *Adv. Mater.*, 2010, **22**, 1369.

5 (a) J. Bill, *Adv. Sci. Technol.*, 2006, **45**, 643; (b) S. Ludwigs, U. Steiner, A. N. Kulak, R. Lam and F. C. Meldrum, *Adv. Mater.*, 2006, **18**, 2270; (c) J. Aizenberg and G. J. Hendler, *J. Mater. Chem.*, 2004, **14**, 2066; (d) K. D. Anderson, M. Luo, R. Jakubiak, R. R. Naik, T. J. Bunning and V. V. Tsukruk, *Chem. Mater.*, 2010, DOI: 10.1021/cm100500d.

6 (a) S. Davis, E. Dujardin and S. Mann, *Curr. Opin. Solid State Mater. Sci.*, 2003, **7**, 273; (b) K. Gorna, R. Munoz-Espi, F. Groehn and G. Wegner, *Macromol. Biosci.*, 2007, **7**, 163; (c) G. Ahmad, M. Dickerson, B. Church, Y. Cai, S. Jones, R. Naik, J. King, C. Summers, N. Kröger and K. H. Sandhage, *Adv. Mater.*, 2006, **18**, 1759.

7 (a) M. B. Dickerson, K. H. Sandhage and R. R. Naik, *Chem. Rev.*, 2008, **108**, 4935; (b) L. A. Estroff, *Chem. Rev.*, 2008, **108**, 4329; (c) Q. Ji, S. Acharya, J. P. Hill, A. Vinu, S. B. Yoon, J. S. Yu, K. Sakamoto and K. Ariga, *Adv. Funct. Mater.*, 2009, **19**, 1792.

8 J. S. Mohammed and W. L. Murphy, *Adv. Mater.*, 2009, **21**, 2361.

9 R. L. Brutchey and D. E. Morse, *Chem. Rev.*, 2008, **108**, 4915.

10 N. Kröger, M. B. Dickerson, G. Ahmad, Y. Cai, M. S. Haluska, K. H. Sandhage, N. Poulsen and V. C. Sheppard, *Angew. Chem., Int. Ed.*, 2006, **45**, 7239.

11 M. Hildebrand, *Chem. Rev.*, 2008, **108**, 4855.

12 D. Bavykin, J. Friedrich and F. Walsh, *Adv. Mater.*, 2006, **18**, 2807.

13 O. Durupthy, J. Bill and F. Aldinger, *Cryst. Growth Des.*, 2007, **7**, 2696.

14 J. L. Sumerel, W. Yang, D. Kisailus, J. C. Weaver, J. H. Choi and D. E. Morse, *Chem. Mater.*, 2003, **15**, 4804.

15 H. R. Luckarift, M. B. Dickerson, K. H. Sandhage and J. C. Spain, *Small*, 2006, **2**, 640.

16 M. J. Pender, L. A. Sowards, J. D. Hartgerink, M. O. Stone and R. Naik, *Nano Lett.*, 2006, **6**, 40.

17 S. Sewell and D. Wright, *Chem. Mater.*, 2006, **18**, 3108.

18 M. B. Dickerson, S. E. Jones, Y. Cai, G. Ahmad, R. R. Naik, N. Kröger and K. H. Sandhage, *Chem. Mater.*, 2008, **20**, 1578.

19 K. E. Cole and A. M. Valentine, *Biomacromolecules*, 2007, **8**, 1641.

20 K. E. Cole, A. N. Ortiz, M. A. Schoonen and A. M. Valentine, *Chem. Mater.*, 2006, **18**, 4592.

21 M. T. Kumara, M. Subra and B. J. Tripp, *J. Nanosci. Nanotechnol.*, 2007, **7**, 2260.

22 K. Sano, S. Yoshii, I. Yamashita and K. Shiba, *Nano Lett.*, 2007, **7**, 3200.

23 C. Jeffryes, T. Gutu, J. Jiao and G. L. Rorrer, *ACS Nano*, 2008, **2**, 2103.

24 X. X. Feng, L. L. Zhang, J. Y. Chen, Y. H. Guo, H. P. Zhang and C. I. Jia, *Int. J. Biol. Macromol.*, 2007, **40**, 105.

25 J. L. Brash and T. A. Horbett, in *Proteins at Interfaces: II. Fundamentals and Applications*, ed. T. A. Horbett, J. L. Brash, Am. Chem. Soc., Washington, DC, 1995, p. 1.

26 S. M. Liu and C. A. Haynes, *J. Colloid Interface Sci.*, 2004, **275**, 458.

27 G. Decher, *Science*, 1997, **277**, 1232.

28 A. J. Chung and M. F. Rubner, *Langmuir*, 2002, **18**, 1176.

29 J. A. Hiller, J. D. Mendelsohn and M. F. Rubner, *Nat. Mater.*, 2002, **1**, 59.

30 P. Hammond, *Adv. Mater.*, 2004, **16**, 1271.

31 Y. Lvov, K. Ariga, I. Ichinose and T. Kunitake, *Langmuir*, 1996, **12**, 3038.

32 S. Srivastava and N. Kotov, *Acc. Chem. Res.*, 2008, **41**, 1831.

33 P. Schwinte, J.-C. Voegel, C. Picart, Y. Haikel, P. Schaaf and B. J. Szalontai, *J. Phys. Chem. B*, 2001, **105**, 11906.

34 T. Boudou, T. Crouzier, K. Ren, G. Blin and C. Picart, *Adv. Mater.*, 2009, **21**, 1.

35 M. Biesalski, J. Rühe, R. Kügler and W. Knoll, in *Handbook of Polyelectrolytes and their Applications*, ed. S. K. Tripathy, J. Kumar, H. S. Nalwa, Am. Sci. Pub., San Diego, 2002, vol. 1, pp. 39–63.

36 T. W. Graul and J. B. Schlenoff, *Anal. Chem.*, 1999, **71**, 4007.

37 C. Picart, G. Ladam, B. Senger, J.-C. Voegel, P. Schaaf, F. J. G. Cuisinier and C. J. Gergely, *Chem. Phys.*, 2001, **115**, 1086.

38 L. Richert, Ph. Lavalle, D. Vautier, B. Senger, J.-F. Stoltz, P. Schaaf, J.-C. Voegel and C. Picart, *Biomacromolecules*, 2002, **3**, 1170.

39 D. S. Salloum and J. B. Schlenoff, *Biomacromolecules*, 2004, **5**, 1089.

40 G. Ladam, P. Schaaf, F. J. G. Cuisinier, G. Decher and J. C. Voegel, *Langmuir*, 2001, **17**, 878.

41 A. Quinn, E. Tjipto, A. Yu, T. R. Gengenbach and F. Caruso, *Langmuir*, 2007, **23**, 4944.

42 L. Szyk, P. Schwinte, J. C. Voegel, P. Schaaf and B. Tinland, *J. Phys. Chem. B*, 2002, **106**, 6049.

43 P. Schwinte, V. Ball, B. Szalontai, Y. Haikel, J.-C. Voegel and P. Schaaf, *Biomacromolecules*, 2002, **3**, 1135.
44 V. Ball, M. Winterhalter, P. Schwinte, Ph. Lavalle, J. C. Voegel and P. Schaaf, *J. Phys. Chem. B*, 2002, **106**, 2357.
45 F. Caruso, D. N. Furlong, K. Ariga, I. Ichinose and T. Kunitake, *Langmuir*, 1998, **14**, 4559.
46 S. A. Sukhishvili and S. Granick, *J. Chem. Phys.*, 1999, **110**, 10153.
47 V. Izumrudov, E. Kharlampieva and S. A. Sukhishvili, *Biomacromolecules*, 2005, **6**, 1782.
48 K. Ariga and T. Kunitake, in *Protein Architecture, Interfacing Molecular Assemblies and Immobilization Biotechnology*; ed. Y. Lvov, H. Möhwald, Marcel Dekker, New York, 2000, p. 169.
49 C. Reichhart and C. Czeslik, *Langmuir*, 2009, **25**, 1047.
50 E. Kharlampieva, T. Tsukruk, J. M. Slocik, H. Ko, N. Poulsen, R. R. Naik, N. Kröger and V. V. Tsukruk, *Adv. Mater.*, 2008, **20**, 3274.
51 E. Kharlampieva, J. M. Slocik, S. Singamaneni, N. Poulsen, N. Kroger, R. R. Naik and V. V. Tsukruk, *Adv. Funct. Mater.*, 2009, **19**, 2303.
52 C. Jiang, S. Markutsya and V. V. Tsukruk, *Adv. Mater.*, 2004, **16**, 157.
53 V. V. Tsukruk and D. H. Reneker, *Polymer*, 1995, **36**, 1791.
54 V. V. Tsukruk, *Rubber Chem. Technol.*, 1997, **70**, 430.
55 S. Singamaneni, M. Gupta, R. Yang, M. M. Tomczak, R. R. Naik, Z. L. Wang and V. V. Tsukruk, *ACS Nano*, 2009, **3**, 2593.
56 Accelrys website, http://accelrys.com/products/materials-studio/.
57 C. Cole, J. D. Barber and G. J. Barton, *Nucleic Acids Res.*, 2008, **36**, W197.
58 J. A. Cuff and G. J. Barton, *Proteins: Struct., Funct., Genet.*, 2000, **40**, 502.
59 FASTA, http://fasta.bioch.virginia.edu/fasta_www2/fasta_list2.shtml.
60 C. Gergely, S. Bahi, B. Szalontai, H. Flores, P. Schaaf, J. C. Voegel and F. J. C. Cuisiner, *Langmuir*, 2004, **20**, 5575.
61 M. Jackson, P. I. Haris and D. Chapman, *Biochim. Biophys. Acta, Protein Struct. Mol. Enzymol.*, 1989, **998**, 75.
62 C. Dicko, D. Knoght, J. M. Kenney and F. Vollrath, *Biomacromolecules*, 2004, **5**, 2105.
63 J. Safar, P. Roller, G. C. Ruben, D. C. Gajdusek and C. J. Gibbs, *Biopolymers*, 1993, **33**, 1461.
64 E. Kharlampieva, D. Pristinski and S. A. Sukhishvili, *Macromolecules*, 2007, **40**, 6967.
65 M. Müller, T. Rieser, P. L. Dubin and K. Lunkwitz, *Macromol. Rapid Commun.*, 2001, **22**, 390.
66 S. V. Patwardhan, R. Maheshwari, N. Mukherjee, K. L. Kiick and S. J. Clarson, *Biomacromolecules*, 2006, **7**, 491.
67 A. Bentaleb, A. Abele, Y. Haikel, P. Schaaf and J. C. Voegel, *Langmuir*, 1998, **14**, 6493.
68 K. Kneipp, H. Kneipp, L. Itzkan, R. R. Dasari and M. S. Feld, *Chem. Rev.*, 1999, **99**, 2957.
69 C. Jiang, W. Y. Lio and V. V. Tsukruk, *Phys. Rev. Lett.*, 2005, **95**, 115503.
70 M. Gotic, M. Ivanda, S. Popovic, S. Music, A. Sekulic, A. Turkovic and K. Furic, *J. Raman Spectrosc.*, 1997, **28**, 555.
71 J. Wang and Z. Lin, *Chem. Mater.*, 2008, **20**, 1257.
72 N. Laugel, J. Hemmerlé, N. Ladhari, Y. Arntz, E. Gonthier, Y. Haikel, J. C. Voegel, P. Schaaf and V. Ball, *J. Colloid Interface Sci.*, 2008, **324**, 127.
73 F. Boulmedais, P. Schwinte, C. Gergely, J. C. Voegel and P. Schaaf, *Langmuir*, 2002, **18**, 4523.
74 M. E. Rousseau, L. Beaulieu, T. Lefèvre, J. Paradis, T. Asakura and M. Pèzolet, *Biomacromolecules*, 2006, **7**, 2512.
75 F. Boulmedais, M. Bozonnet, P. Schwinté, J.-C. Voegel and P. Schaaf, *Langmuir*, 2003, **19**, 9873.
76 B. W. Hu, P. Zhou, I. Noda and Q. X. Ruan, *J. Phys. Chem. B*, 2006, **110**, 18046.
77 X. H. Zong, P. Zhou, Z.-Z. Shao, S.-M. Chen, X. Chen, B.-W. Hu, F. Deng and W. H. Yao, *Biochemistry*, 2004, **43**, 11932.
78 X. Chen, D. P. Knight and Z. Shao, *Soft Matter*, 2009, **5**, 2777.
79 E. Kharlampieva, D. Zimnitsky, M. Gupta, K. N. Bergman, D. L. Kaplan, R. R. Naik and V. V. Tsukruk, *Chem. Mater.*, 2009, **21**, 2696.
80 J. G. Hardy, L. M. Römer and T. H. Scheibel, *Polymer*, 2008, **49**, 4309.
81 J. Safar, P. P. Roller, G. C. Ruben, D. C. Gajdusek and C. J. Gibbs, *Biopolymers*, 1993, **33**, 1461.
82 C. P. O'Brien, S. J. Stuart, D. A. Bruce and R. A. Latour, *Langmuir*, 2008, **24**, 14115.
83 L. Lenoci and P. Camp, *J. Am. Chem. Soc.*, 2006, **128**, 10111.